Sensors and Actuators A 276 (2018) 176–185

Contents lists available at ScienceDirect

Sensors and Actuators A: Physical

journal homepage: www.elsevier.com/locate/sna

The influence of tube wall on fluid flow, permeability and streaming potential in porous transducer for liquid circular angular accelerometers

Siyuan Cheng[a,b,*], Mengyin Fu[a], Meiling Wang[a], F.A. Kulacki[b]

[a] School of Automation, Beijing Institute of Technology, Beijing, 100081, China
[b] Department of Mechanical Engineering, University of Minnesota, Minneapolis, MN, 55455, the United States

ARTICLE INFO

Article history:
Received 20 December 2017
Received in revised form 10 April 2018
Accepted 11 April 2018
Available online 18 April 2018

Keywords:
Angular accelerometer
Wall effect
Porous transducer
Capillary bundle model
Streaming potential

ABSTRACT

The effects of the tube wall on the fluid flow, permeability and streaming potential are reported for a porous transducer for use in a liquid circular angular accelerometer. Fluid flow and pressure near the surface of the transducer are modeled and validated numerically. We show that the differential pressure across the transducer is not affected by the tube wall. A capillary bundle model is employed to represent the transducer to obtain the radial porosity, permeability and streaming potential distributions due to wall effects. A simulated spherical packing is generated from measured particle parameters to specify the model by calculating the radial porosity distribution. The theoretical permeability and streaming potential coupling coefficient are located within one standard deviation from the mean of measurements. Due to the radial distribution of streaming potential, the electrode can be configured into a large streaming potential region to measure the signal more efficiently. Three electrode configurations are described based on these results, which can be applied to increase the signal of the sensor.

1. Introduction

Angular accelerometers play an important role in angular acceleration measurement, which can be used in navigation, robotics and industrial machines [1–7]. To obtain no-delay and accurate angular acceleration, different angular accelerometers have been designed and investigated [8–18]. Traditional solid-based angular accelerometers yield great precision, but their bandwidth and range are limited [8,9]. Novel micro-electro-mechanical systems (MEMS) technologies bring new possibilities to this field because of the miniaturization of the angular sensor [10]. The reduced inertia of the sensor produces improvements in bandwidth and range but with unsatisfactory accuracy. New categories of angular accelerometer have been investigated recently, employing electromagnetics [11], heat transfer [12], and fluidics [13–18]. Compared to other angular accelerometers, fluidic accelerometers have attracted much attention owing to their good accuracy, bandwidth, range, size, and insensitivity to linear acceleration [13–18].

The design and operating principle of a liquid circular angular accelerometer (LCAA) have been recently reported [15–19]. The LCAA has a structure typical of fluidic angular accelerometers (Fig. 1(a)). A viscous fluid flows in a circular tube made of glass, and a porous transducer sintered by glass microspheres is fixed in the circular tube. In theory, signal generation of an LCAA can be divided into fluidic and electrokinetic processes (Fig. 1(b)) [15]. Owing to the fluid motion, the angular acceleration input, β, is transformed into differential pressure across the transducer, ΔP. In the electrokinetic process, owing to the existence of the electrical double layer at the interface between the transducer and the fluid, a differential pressure results in the movement of the electrical charge and the generation of a streaming potential signal, E_s, [20,21]. Electrodes mounted on the two sides of the transducer measure the streaming potential.

In [15], a transfer function of the fluidic process has been investigated, which performs accurate prediction in low-frequency gain, $\Delta P/\beta$, but shows large deviation in bandwidth. The transient fluid in the circular tube was then modeled with the consideration of fluid compressibility [16], which can be used to obtain the frequency response of the fluidic process. This model has been improved, and the influence of structural parameters on the frequency and transient responses of the fluidic process have been reported [17]. The electrokinetic process in the porous transducer is modeled with a streaming potential coupling coefficient (SPCC), $C_{sp} = E_s/\Delta P$, and is illustrated by Helmholtz-Smoluchowski (HS) equation in steady flow [20,22–24]. Because the SPCC shows great

* Corresponding author. Present address: Department of Mechanical Engineering, University of Minnesota, Minneapolis, MN, 55455, the United States.
E-mail address: cheng901229@bit.edu.cn (S. Cheng).

https://doi.org/10.1016/j.sna.2018.04.016
0924-4247/

Nomenclature

A	Cross-section area of the transducer (m^2)
C_f	Factor of viscous resistance in the transducer (1/s)
C_j	Factor inertial resistance in the transducer (1/m)
C_{sp}	Streaming potential coupling coefficient (V/Pa)
C_{sp_core}	Streaming potential coupling coefficient in core region (V/Pa)
d	Diameter of the microspheres (m)
$\bar{d}_p$	Average diameter of the microspheres (m)
d_{ij}	Distance between the centers of the ith and jth spheres (m)
d_{ik}	Distance between the ith sphere and the kth wall (m)
D	Diameter of the circular tube (m)
E_s	Streaming potential (V)
$E\left(r_c^2, r\right)$	Second original moment of rc on every r (m^2)
$\vec{f}_p$	Permeation resistance (m/s^2)
F	Formation factor (non-dimensional)
F_{ij}^c	Elastic force between the ith and jth spheres (N)
F_{ik}^b	Elastic force from the wall (N)
I_s	Streaming current (A)
I_c	Conduction current (A)
I_i	Moment of inertia of the ith sphere ($kg{\cdot}m^3$)
K	Bulk permeability (m^2)
K_{core}	Bulk permeability in core region (m^2)
l_{ij}^c and l_{ik}^b	The distance between F_{ij}^c as well as F_{ik}^b and their contact points on the sphere surface (m)
L	Axial length of the transducer (m)
L_c	Path length of the capillaries (m)
m	Cementation exponent (non-dimensional)
m_i	Mass of the $i$thth sphere (kg)
$n(r_c, r)$	Number density of capillary tubes with radius r_c at r ($1/m^2$)
N_c	Number of the capillary tubes on every r (1/m)
p	Pressure (Pa)
ΔP	Differential pressure across the transducer (Pa)
Q	Volumetric flow rate (m^3/s)
r_c	Capillary radius (m)
r_{min}	Minimal radii of the capillaries (m)
r_{max}	Maximal radii of the capillaries (m)
r_i	Radii of the ith sphere (m)
R	Cross-sectional radius of the circular tube (m)
R_0	Coefficients of fitting function, Eq. (29) (non-dimensional)
$R_e = \rho v_z D/\eta$	Reynolds number
r, θ, z	Cylindrical coordinates, Fig. 1
$\vec{v} = (v_r, v_\theta, v_z)$	Superficial velocity (m/s)
$V(r)$	Total volume at r in transducer (m^3)
$V_f(r)$	Fluid volume at r in transducer (m^3)
α_i	Acceleration of the ith sphere (m/s^2)
$\sim\alpha_1 - \sim\alpha_6$	Coefficients of fitting function, Eq. (29), (non-dimensional)
β	Angular acceleration input (rad/s^2)
β_i	The angular acceleration of the ith sphere (rad/s^2)
$\varepsilon_0, \varepsilon_r$	Vacuum and relative dielectric constants of liquid (F/m, non-dimensional)
ς	Zeta potential on liquid-solid interface (V)
Θ	Transform value from d to r_c (non-dimensional)
μ_d, σ_d	Mean and variance of particle size distribution (non-dimensional)
μ_c, σ_c	Mean and variance of capillary radius distribution (non-dimensional)
ρ	Density of liquid (kg/m^3)
Σ	Total conductance of capillary tubes (S)
Σ_s	Specific surface conductance of capillary tubes (S)
σ_0	Bulk electrical conductivity of liquid (S/m)
η	Dynamic viscosity of liquid (Pa·s)
$\tau = L_c/L$	Capillary tortuosity
φ	Porosity (non-dimensional)
φ_0	Coefficients of fitting function, Eq. (29), (non-dimensional)
$\bar{\varphi}$	Average porosity

dependence on permeability [21,22,24], the permeability of the transducer in the LCAA has been investigated in [18,19]. However, when a porous medium is fixed in a small diameter tube, as in the LCAA, the inner wall of the tube (tube wall) creates a radial distribution of porosity and permeability [25,26], which can further influence the electrokinetic process which is the focus of our investigation. We consider flow in a neighborhood of the transducer and regard the tube as straight (Fig. 1(c)), because the tube radius (Fig. 1(a)) is much larger than the diameter of transducer, D, and the asymmetry of the flow caused by the curvature of the tube can be ignored due to the low Reynolds number [27].

Two factors must be investigated to study the influence of the tube wall. First, the flow in the tube can be modeled as Poiseuille flow [28]. The velocity distribution possibly produces a distribution of the differential pressure across the transducer [29], which will affect the streaming potential. Secondly, because the transducer is essentially a granular porous medium fixed in the tube, the

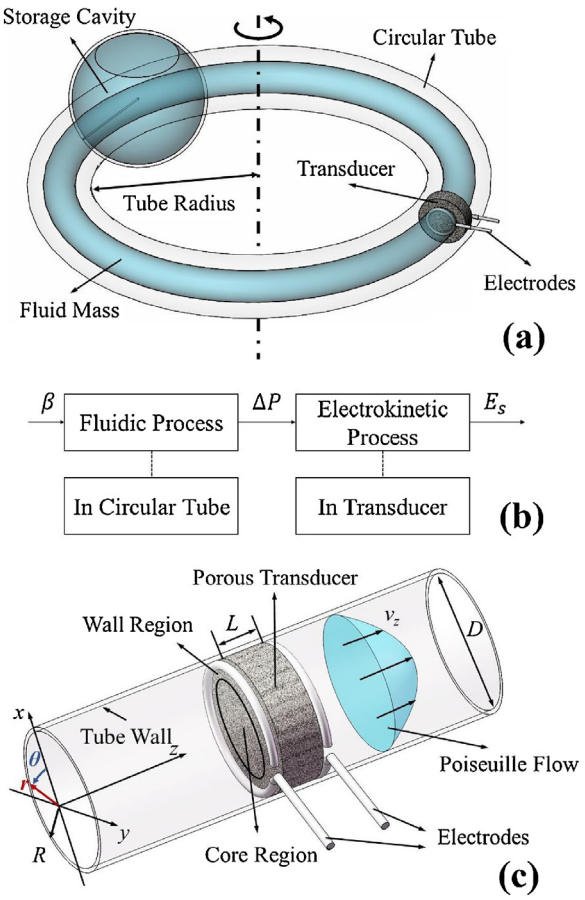

Fig. 1. (a) Sensor structure. (b) Signal generation in LCAA. (c) Fluid flow in the tube with cylindrical coordinates.